

DISPERSION MATCHING WITH SPACE CHARGE IN MESA

A. Khan*, O. Boine-Frankenheim, Technische Universität Darmstadt, Germany
 K. Aulenbacher, Johannes Gutenberg-Universität Mainz, Germany

Abstract

For intense electron bunches traversing through bends, as for example the recirculation arcs of an Energy-Recovery Linac (ERL), dispersion matching with space charge of an arc into the subsequent radio-frequency (RF) structure is essential to maintain the beam quality. We show that beam envelopes and dispersion along the bends and recirculation arcs of an ERL, including space charge forces, can be matched to adjust the beam to the parameters of the subsequent section. The present study is focused on a small-scale, double-sided recirculating linac Mainz Energy-recovering Superconducting Accelerator (MESA). MESA is an under construction two pass ERL at the Johannes Gutenberg-Universität Mainz, which should deliver a continuous wave (CW) beam at 105 MeV for physics experiments with a pseudo-internal target. In this work, a coupled transverse-longitudinal beam matrix approach for matching with space charge in MESA is employed.

INTRODUCTION

For intense electron bunches at low to medium energy traversing through bends, it is essential to understand the details of space-charge-induced effects to maintain beam quality throughout the ERL operation [1]. Particularly, current dependent dispersion matching of an arc into the subsequent RF section has been found to be essential to preserve the beam quality. Dispersion matching with space charge has been discussed mostly in the context of high intensity beams in conventional synchrotrons [2]. For example, [3, 4] outlined the concept of two different dispersion functions, one for the beam center, which is not affected by space charge, and one for the off-center particles. Experiments related to space charge and dispersion with low energy proton beams were performed in the CERN PS Booster, matching the beam from the linac into the synchrotron. Although the space charge was found to be relevant, it was sufficient to use the zero-intensity dispersion for the matching of the beam center, in order to improve the injection efficiency [5]. In this work, we show that the space-charge-modified dispersion plays a key role for the adjustment of the R_{56} required for both the isochronous and the non-isochronous recirculation mode of an ERL.

An important role of the recirculation arc in an ERL is to provide path length adjustment options to set the accurate required RF phase of 0° to 180° for acceleration and deceleration. Transverse space charge modifies the dispersion function along the arc and so the momentum compaction which is the transport matrix element R_{56} for the individual particles. In case the arc settings are chosen for zero-intensity,

one would end up with a dispersion and bunch length different from the design values at a subsequent RF structure [6]. It is therefore necessary to understand the modification of dispersion due to space charge along the arc in order to do proper matching into the next lattice section. Longitudinal space charge also plays an important role, especially for short bunches and small momentum deviations. Longitudinal space-charge-induced variations in the bunch length or momentum deviation also affect the transverse space charge force by varying the local current density and the transverse beam size through the dispersion.

DISPERSION WITH SPACE CHARGE

In the presence of bending magnets, the horizontal displacement x of a particle from the reference particle is written as [6]

$$x(s) = x_\beta(s) + D_0(s)\delta, \quad (1)$$

where x_β is the betatron oscillation amplitude, $D_0 \equiv D_0(s)$ is the dispersion function, and $\delta = \Delta p/p_0$ is the fractional momentum deviation. The linear dispersion function without space charge $D_0(s)$ is the solution of the equation [2]:

$$D_0''(s) + \kappa_x(s)D_0(s) = \frac{1}{\rho(s)}, \quad (2)$$

which gives the local sensitivity of the particle trajectory to the fractional momentum deviation δ , and the prime denotes derivative with respect to distance s along the beamline. ρ is the bending radius and κ_x is the linearized horizontal external focusing gradient.

With space charge, we can write:

$$x_{sc}(s) = x_{sc,\beta}(s) + D\delta, \quad (3)$$

where $D \equiv D(s)$ is the dispersion function with space charge.

Taking the average of Eq. (1) and Eq. (3) and subtracting them over the symmetrical phase space distribution, such that $\langle x_\beta \rangle = \langle x_{sc,\beta} \rangle = 0$, we obtain (see also [4]):

$$\langle x_{sc} \rangle - \langle x \rangle = (D - D_0)\langle \delta \rangle. \quad (4)$$

For a beam with a momentum distribution centered at the design momentum the dispersion describing the position of the beam centroid is space charge independent. This also explains the experimental results obtained in the CERN PS Booster [5]. There the dispersion was measured and matched by changing the beam momentum and recording the displacement of the beam center.

To observe the effect of space charge on the individual particle dispersion, we have to compute the second moments of the beam distribution. Using the assumption that the momentum deviation is uncorrelated to the betatron oscillations,

* khan@temf.tu-darmstadt.de

such that $\langle x_{\beta}\delta \rangle = \langle x_{sc,\beta}\delta \rangle = 0$, we get the expression for D by multiplying Eq. (3) by δ and taking the average over the phase space. Following a similar procedure for D' [6]:

$$D = \frac{\langle x_{sc}\delta \rangle}{\langle \delta^2 \rangle} = \frac{\sigma_{16}}{\sigma_{66}}, \quad D' = \frac{\langle x'_{sc}\delta \rangle}{\langle \delta^2 \rangle} = \frac{\sigma_{26}}{\sigma_{66}}. \quad (5)$$

where the last equalities are written in terms of the beam sigma matrix [3, 6] as explained following.

Instead of individual particle tracking, we track the rms beam envelope defined as [3, 7, 8]:

$$\sigma_{ij} = \langle u_i u_j \rangle \quad (6)$$

where the averages are taken over the phase space variables and the subscripts i, j run from 1 to 6 representing x, x', y, y', z, z' . The time evolution of a beam matrix σ_s from s_0 to s_1 along the longitudinal position s is given by [3, 8]

$$\sigma_{s_1} = R(s_0 \rightarrow s_1) \sigma_{s_0} R^T(s_0 \rightarrow s_1), \quad (7)$$

where R is the transport matrix. The space charge kick is implemented as $R(s_0, s_0 + \Delta s) = R_{\Delta s} R^{SC}$, where $R_{\Delta s}$ is a drift of length Δs and R^{SC} is the space charge kick as described in Ref. [3, 8, 9].

The effective transverse rms beam radii X and Y including dispersion are:

$$X^2 = \sigma_x^2 + D_x^2 \sigma_\delta^2, \quad Y^2 = \sigma_y^2 + D_y^2 \sigma_\delta^2, \quad (8)$$

where $\sigma_x = \sqrt{\langle x^2 \rangle} = \sqrt{\sigma_{11}}$, $\sigma_y = \sqrt{\langle y^2 \rangle} = \sqrt{\sigma_{33}}$ are the rms betatron amplitudes, and $\sigma_\delta = \sqrt{\langle \delta^2 \rangle} = \sqrt{\sigma_{66}}$ is the rms momentum deviation.

The momentum compaction R_{56} is the variation of the path length with momentum deviation for a relativistic beam:

$$R_{56} = \frac{\Delta L}{\delta} = \int_0^L \frac{D_x + D_y}{\rho} ds, \quad (9)$$

which also is the (5,6)th component of the 6×6 transport matrix of the beamline elements. Where L is the total path length of the beamline.

In a beamline with dispersion D , space charge modifies the path length or time of flight of individual particles following the space charge dependent phase slip factor η :

$$\eta = \left. \frac{R_{56}}{L} \right|_{s=L} \quad (10)$$

In this work, we use above discussed beam matrix approach to obtain the optical functions along a beamline with bends, including the self-consistent space charge force.

OVERVIEW OF MESA

An overview of the MESA facilities is shown in Fig. 1. The electron source provides up to 1 mA of a polarized beam

at 100 keV. In the next planned stage of MESA, the electron source will provide 10 mA of unpolarized beam current. This electron source is followed by a spin manipulation system containing two Wien filters. A chopper and two buncher cavities prepare the bunches for the normal-conducting milliamperere booster (MAMBO), which accelerates them to 5 MeV. In MESA electrons will be accelerated by two ELBE-type cryomodules each housing two superconducting TESLA-type cavities with an accelerating gradient of 12.5 MeV, which results in 25 MeV per pass. There are four spreader sections for separating and recombining the beam and two chicanes for injection and extraction of the 5 MeV beam.

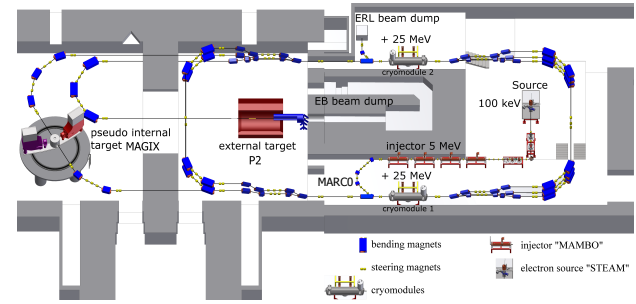


Figure 1: A schematic layout of MESA.

MESA is planned to operate in two modes: external beam (EB) mode and energy-recovery (ER) mode. In EB mode, the electron beam will gain 155 MeV with up to 150 μ A beam current by circulating thrice around the accelerator. The beam is planned to be used for high-precision fixed-target experiments. The main experiment in the EB mode will be the measurement of the electroweak mixing angle at the P2 setup [10]. Similarly in ER mode, the CW electron beam will gain 105 MeV with 1(10) mA beam current by circulating twice around the accelerator. The main experiments in the ER mode will be pseudo-internal target (PIT) experiments in a search for dark photons with high luminosity [11]. In ER mode, 100 MeV of the beam energy can be recovered by decelerating the beam in the superconducting cavities and using this recovered energy to accelerate further bunches [12]. Both operational modes set high demands on beam quality and stability. Mainly, a low momentum deviation is required to achieve higher precision of experiments. The main prerequisite for sustaining beam quality is a proper beam transport through the injection arc (MARCO), which is a 5 MeV, 180°, first-order achromat with flexible 1st order momentum compaction R_{56} required for the different isochronous and non-isochronous recirculation modes.

SIMULATION RESULTS

In this section, we present the solutions for the beam envelopes, dispersion and momentum compaction with space charge in MESA. Estimation of space charge effects is done for a typical set of beam parameters listed in Table 1 [6]. Note that we are using an idealized lattice for the MESA beamline ignoring magnet misalignments and multipole er-

Content from this work may be used under the terms of the CC BY 3.0 licence (© 2019). Any distribution of this work must maintain attribution to the author(s), title of the work, publisher, and DOI

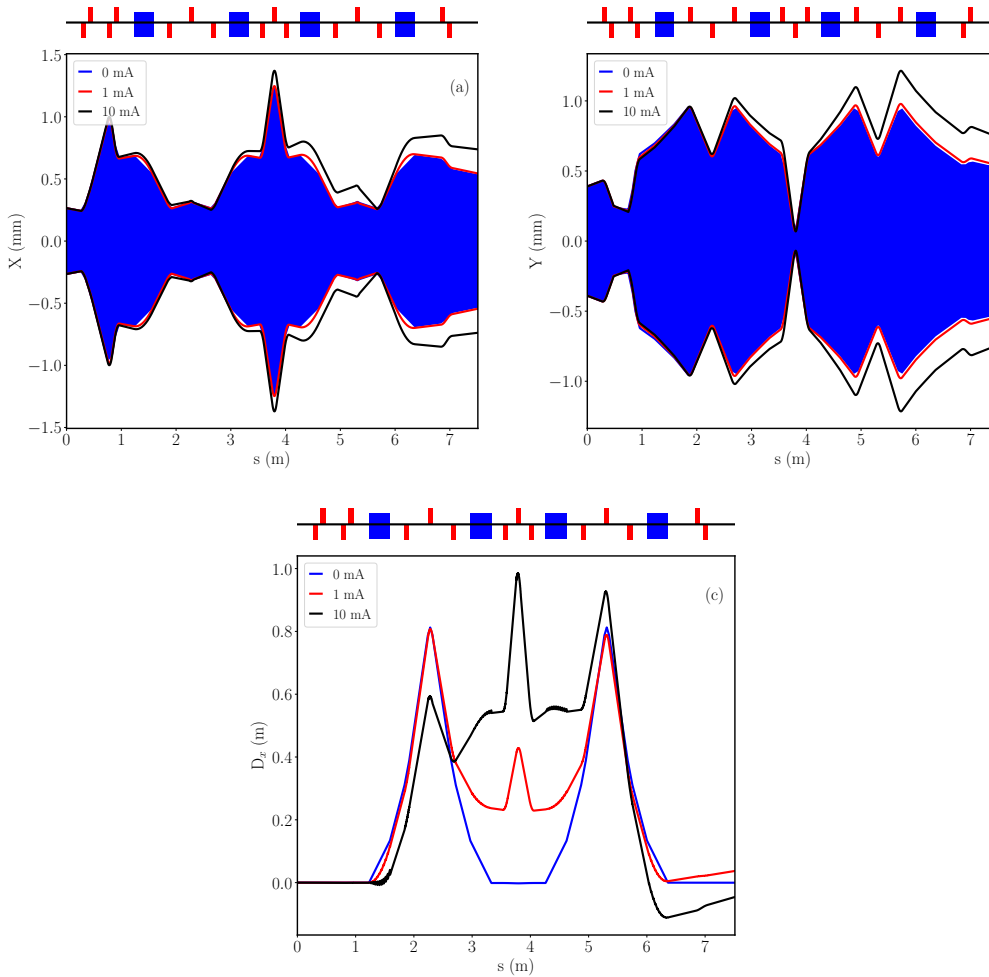


Figure 2: Evolution of (a) horizontal beam envelope, (b) vertical beam envelope, (c) dispersion, and (d) momentum compaction along the MARCO beamline for $I = 0, 1, 10$ mA including transverse and longitudinal space charge.

rors for the simulations. Additional studies are required to include these effects.

First, we compute the horizontal and vertical beam envelope, and dispersion profile along the MARCO arc for “zero”, 1, and 10 mA current and an rms momentum deviation of 10^{-4} , accounting for coupled transverse-longitudinal space charge. The injection arc of MESA (MARCO) is suppose to be a dual purpose 5 MeV arc with finite momentum compaction R_{56} for energy recovery and external beam mode. A nominal design of arc should deliver fixed beam parameters with zero dispersion after first cryomodule for energy recovery operation. Figures 2 (a)–(b) show the variation of horizontal and vertical transverse envelopes along s , for $I = 1$, and 10 mA in MARCO. It can be seen from Fig. 2 (c) that with longitudinal and transverse space charge the dispersion is significantly modified for non-zero currents. The sign reversal of D_x may contribute to phase mismatch at the entrance of the RF section due to changes in the time of flight of particles (see Eq. (9) and Eq. (10)). Thus, it is important

to consider both longitudinal and transverse space charges for optimal matching.

Table 1: Beam Parameters for the Injection Arc of MESA.

Parameters [unit]	Symbol	Value
Kinetic energy [MeV]	E_k	5
Bunch charge [pC]	Nq	0.77/7.7
RF frequency [GHz]	f_{rf}	1.3
RMS momentum deviation [%]	σ_δ	0.01
Half bunch length [ps]	z_m	4.2
Normalized emittance [π mm mrad]	$\epsilon_{nx,ny}$	2/6
Momentum compaction [m]	R_{56}	0.14

Second, we compute the beam envelopes and dispersion along the full MESA beamline to observe the effect of space charge mismatch. Figure 3 (a)–(b) shows the horizontal and vertical beam envelopes with space charge for $I =$ “zero”, 1, and 10 mA in MESA. It can be seen from Fig. 3 (c)–(d) that dispersion with space charge is significantly modified

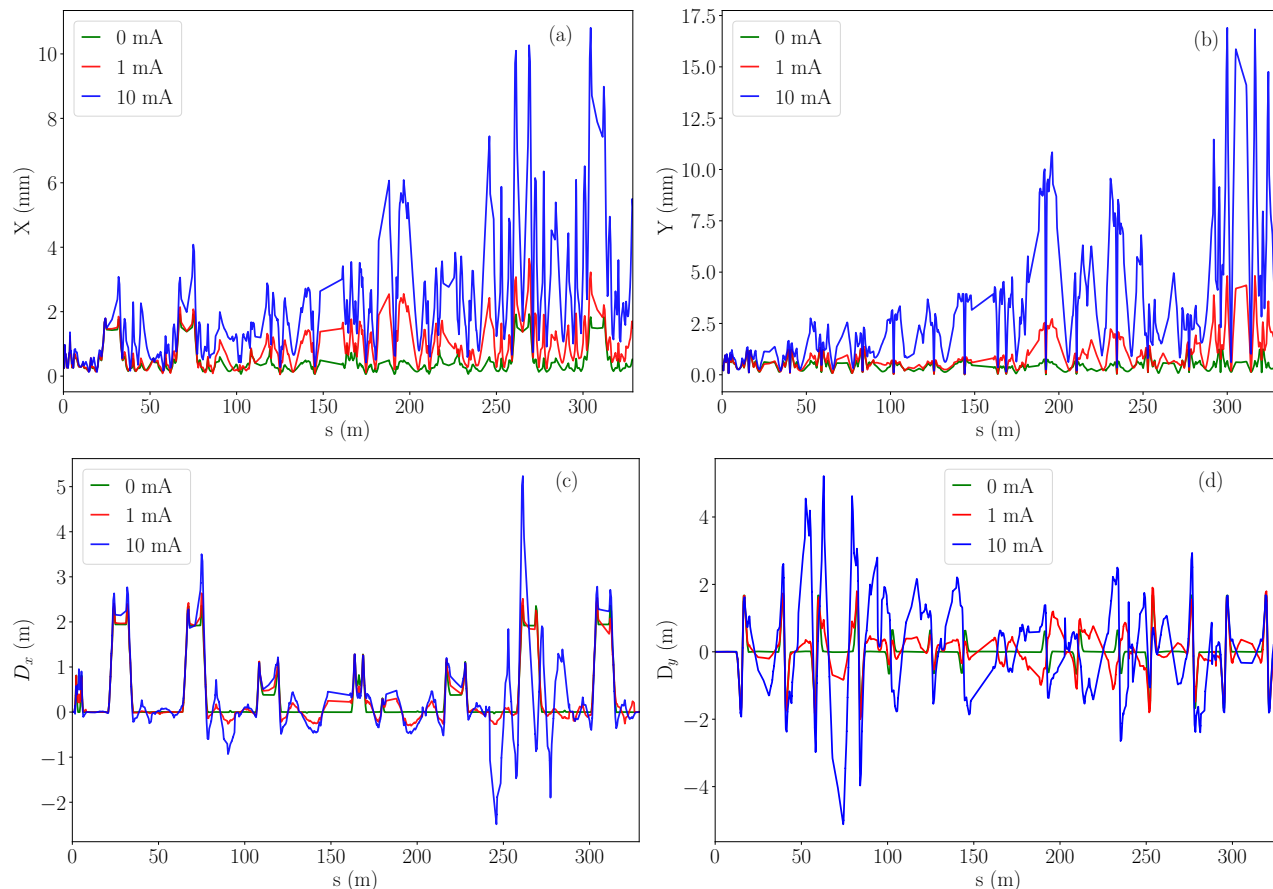


Figure 3: Evolution of (a) horizontal beam envelope, (b) vertical beam envelope, (c) horizontal dispersion function, and (d) vertical dispersion function along the MESA beamline for $I = 0, 1, 10$ mA including transverse and longitudinal space charge.

for non-zero currents from the designed values. Also, there appears to be a strong mismatch in the beam envelopes and dispersion near PIT experiment at $s = 175$ m and in the further arcs. This strong effect of space charge at high-energy arc (105 MeV) can be expected from Fig. 2 results that space charge induces a mismatch between the beam envelopes and non-zero dispersion at the end of the 5 MeV low energy injection arc which leads to the strong mismatch in the beam envelopes in the further arcs during acceleration and deceleration and distorts the phase space.

In this work, we optimize the lattice parameters of MARCO to get fixed values of $\beta_{x,y}$, $\alpha_{x,y}$, D_x , D'_x and R_{56} at the end so we can estimate the mismatch in the beam envelopes and dispersion in the further arcs. While the transverse dispersion functions D_x and D'_x need to be zero at the end of the arc, the longitudinal dispersion is fixed at a finite value of $R_{56} = 0.14$ m in order to use the arc as part of a bunch compressor to achieve a short bunch length at the start of the first superconducting RF section.

As can be seen from Fig. 2, MARCO consists of two double-bend achromats (DBA) [13]. It controls both transverse beam confinement and longitudinal phase space to compress the bunch. A set of four quadrupoles at the start of

the arc matches the first DBA to the MAMBO injector. The central part of the arc between the two DBAs contains three quadrupoles to again match the Twiss parameters. A total of 15 quadrupole gradients are available knobs to optimize the lattice.

Table 2: Example current, the horizontal and vertical beta functions mismatch respectively, and the horizontal dispersion mismatch from the design value at the end of MARCO with space charge [6].

I (mA)	$\frac{\Delta\beta_x}{\beta_x}$ ($\%$)	$\frac{\Delta\beta_y}{\beta_y}$ ($\%$)	ΔD_x (m)
1	3.0	2.6	0.037
5	17.5	17.3	-0.017
10	39.7	41.0	-0.046
10 (matched)	0	0	0

Table 2 illustrates the horizontal beta function mismatch $\Delta\beta_x/\beta_x$ and the vertical beta function $\Delta\beta_y/\beta_y$ mismatch from the design value respectively, and the horizontal dispersion mismatch ΔD_x from the design value at the end of MARCO with space charge for 1, 5 and 10 mA. Here, $\Delta\beta_x = \beta_{sc,x} - \beta_x$, $\Delta\beta_y = \beta_{sc,y} - \beta_y$, and $\Delta D_x = D_{sc,x} - D_x$. We can see from the last column of Table 2 that current de-

Content from this work may be used under the terms of the CC BY 3.0 licence (© 2019). Any distribution of this work must maintain attribution to the author(s), title of the work, publisher, and DOI

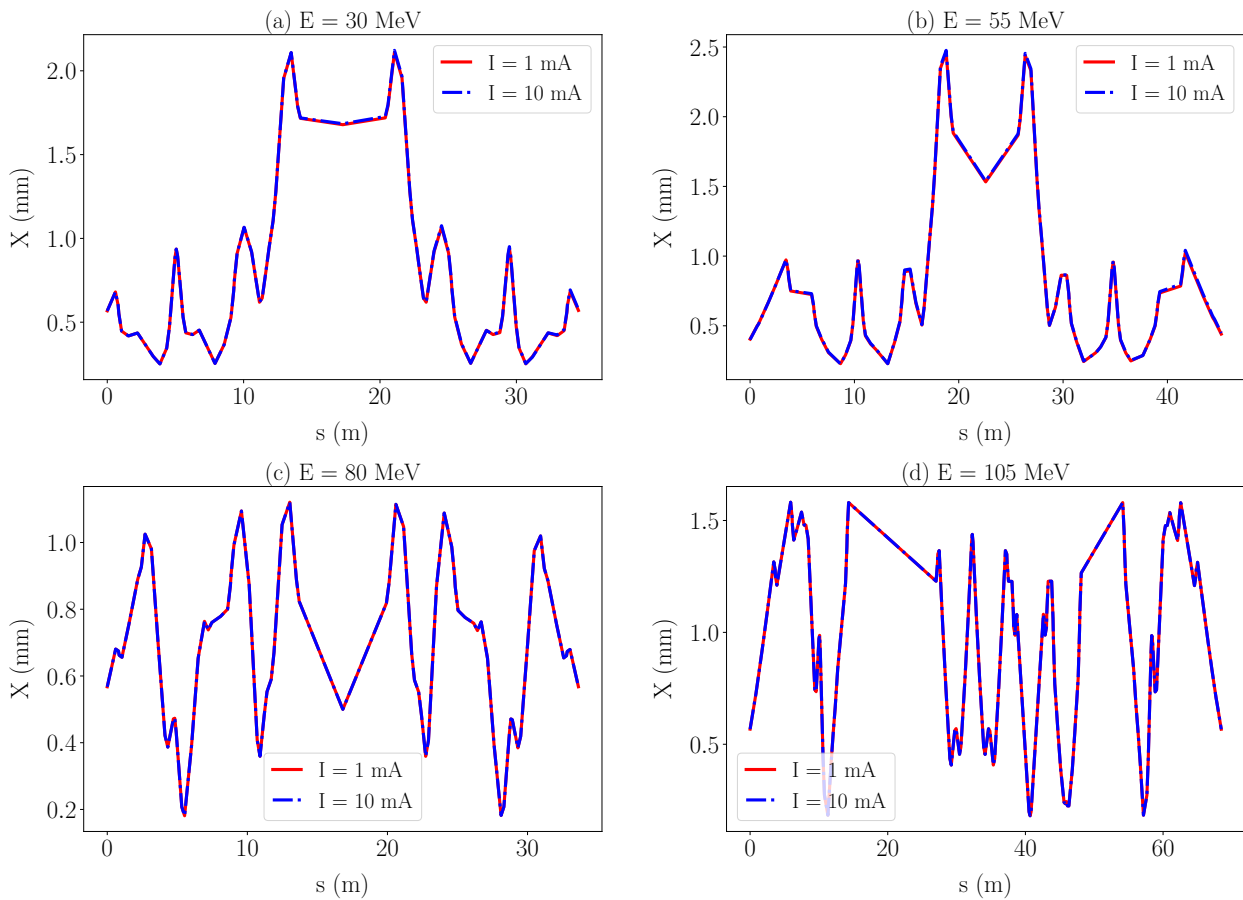


Figure 4: Horizontal beam envelopes along the (a) 30 MeV recirculation arc (b) 55 MeV recirculation arc (c) 80 MeV recirculation arc, (d) 105 MeV internal arc of MESA for $I = 1, 10$ mA when the beam is matched with space charge in the 5 MeV injection arc MARC0.

pendent dispersion is non-zero at the end of MARC0 which might lead to emittance growth in the RF section because of longitudinal-transverse phase space coupling.

We use a simple “random walk” routine to optimize all lattice parameters to get the matched solution of MARC0 with space charge. Note that D' should be considered for optimization of D in the beamline with space charge. D' must be zero at the central quadrupole of the achromat to achieve zero dispersion at the end of the last dipole. A new set of quadrupole strengths is obtained with corrections of up to 15% in the original quadrupole to get the matched solution.

The above results show the beam envelopes and dispersion mismatch from the design values due to space charge effects. Thus, to estimate the intensity limitations due to space charge in MESA, first we match the beam in the MARC0 using the random walk scheme as discussed above, and then track that matched beam through high energy recirculation arcs. Figure 4 shows the horizontal beam envelopes along the 30, 55, 80, and 105 MeV recirculation arcs of MESA for $I = 1, 10$ mA when the beam is matched with space charge at the MARC0. It can be seen that if all the lattice parameters of the beamline are matched properly with the subsequent RF

structure in the presence of space charge at the injection, there is no mismatch between the beam envelopes due to space charge in the high-energy recirculations arcs of MESA.

CONCLUSION

This study shows that the proper matching of the injection arc into the RF section of an ERL is important with space charge. We showed how space charge modifies the dispersion function along the arc and so the momentum compaction which leads to change in the path length of electrons. A “random walk” scheme was employed to get the matched parameters with space charge at the subsequent RF section of an arc. In subsequent recirculation arcs of MESA, the beam energy is much higher than the injection energy. It is shown that MESA has no intensity limitations due to space charge if the beam is properly matched with space charge at the injection. The future application of this work is to predict the longitudinal space-charge-induced microbunching instability in MESA, which depends on the details of the dispersion function along the arcs [14].

REFERENCES

- [1] Aamna Khan, Kurt Aulenbacher, and Oliver Boine-Frankenheim. “Study of microbunching instability in MESA”. In *59th ICFA Advanced Beam Dynamics Workshop on Energy Recovery Linacs (ERL’17)*, 2018. doi:10.18429/JACoW-ERL2017-THICCC002.
- [2] Martin Reiser. “Theory and design of charged particle beams”. John Wiley & Sons, 2008. ISBN: 978-3-527-40741-5.
- [3] Tomohiro Ohkawa and Masanori Ikegami. “Dispersion matching at the injection from a high-intensity linac to a circular accelerator”. *Nuclear Instruments and Methods in Physics Research Section A*, 576(2-3):274–286, 2007. doi:10.1016/j.nima.2007.03.015.
- [4] S. Bernal, B. Beaudoin, T. Koeth, and P. G. O’Shea. “Smooth approximation model of dispersion with strong space charge for continuous beams”. *Physical Review Special Topics - Accelerators and Beams*, 14(10):1–15, 2011. doi:10.1103/PhysRevSTAB.14.104202.
- [5] K. Hanke, J. Sanchez-Conejo, and R. Scrivens. “Dispersion matching of a space charge dominated beam at injection into the CERN PS Booster”. *Proceedings of the 2005 Particle Accelerator Conference*, p. 3283, 2005, paper: TPAT054.
- [6] Aamna Khan, Oliver Boine-Frankenheim, Florian Hug, and Christian Stoll. “Beam matching with space charge in energy recovery linacs”. *Nuclear Instruments and Methods in Physics Research Section A*, 948, p. 162822, 2019. doi:10.1016/j.nima.2019.162822.
- [7] Thomas P Wangler. “RF Linear accelerators”. John Wiley & Sons, 2008. ISBN:978-3-527-40680-7.
- [8] Kenneth R Crandall. “TRACE 3D documentation”. Technical report, Los Alamos National Lab., 1987.
- [9] Christopheer K Allen and N Pattengale. “Theory and technique of beam envelope simulation”. Los Alamos National Laboratory, Internal Report LA-UR-02-4979, 2002.
- [10] Dominik Becker, Razvan Bucoveanu, Carsten Grzesik, and et al. “The P2 experiment”. *The European Physical Journal A*, 54(11):208, Nov 2018. doi:10.1140/epja/i2018-12611-6.
- [11] Achim. Denig. “Recent results from the Mainz Microtron MAMI and an outlook for the future”. *AIP Conf.Proc.*, 1735. 020006, 2016. doi:10.1063/1.4949374.
- [12] Kurt Aulenbacher. “Opportunities for parity violating electron scattering experiments at the planned MESA facility”. *Hyperfine Interactions*, 200(1-3):3–7, 2011. doi:10.1007/s10751-011-0269-9.
- [13] Helmut Wiedemann. “Particle accelerator physics”. Springer, 2015. doi:10.1007/978-3-319-18317-6.
- [14] A. Khan, O. Boine-Frankenheim, and C. Stoll. “Space charge and microbunching studies for the injection arc of MESA”. In *Journal of Physics: Conference Series*, 1067, p. 062022, 2018. doi:10.1088/1742-6596/1067/6/062022.